International Journal of Nanomedicine

Dovepress
Taylor & Francis Group

Open Access Full Text Article

ORIGINAL RESEARCH

Ameliorative Hypoglycemic Effect of 1-DNJ via Structural Derivatization Followed by Assembly Into Selenized Nanovesicles

Shuxian Ruan[1,*], Yanli Du[2,*], Xianyuan Zhang[3], Xingwang Zhang[1], Hao Kang[4]

[1]Department of Pharmaceutics, College of Pharmacy, Jinan University, Guangzhou, People's Republic of China; [2]The First Affiliated Hospital of Jinan University, Guangzhou, People's Republic of China; [3]Meizhou Baoyuantang Pharmaceutical Co., Ltd, Meizhou, People's Republic of China; [4]Department of Medicinal Chemistry and Pharmaceutical Analysis, Anhui College of Traditional Chinese Medicine, Wuhu, People's Republic of China

*These authors contributed equally to this work

Correspondence: Xingwang Zhang; Hao Kang, Email zhangxw@jnu.edu.cn; kanghao@ahzyygz.edu.cn

Purpose: 1-Deoxynojirimycin (1-DNJ), a phytomedicine derived from mulberry leaves and certain bacteria, can inhibit α-glycosidase activity and alleviate insulin resistance, thereby lowering blood glucose levels. However, its short half-life and limited in vivo residence compromise its therapeutic efficacy. This study aimed to optimize the structure of 1-DNJ and develop nano-formulation to ameliorate its pharmacokinetic properties and therapeutic effects.

Methods: We synthesized *N*-oleoyl-1-DNJ (*N*-1-DNJ) and formulated it into selenized nanovesicles using a thin-film hydration method combined with in situ reduction.

Results: The resulting *N*-1-DNJ-loaded selenized nanovesicles (*N*-1-DNJ-Se@NVs) exhibited improved physiological stability and sustained release compared to non-selenized versions. In vivo pharmacokinetic studies in GK rats revealed that *N*-1-DNJ-Se@NVs presented prolonged absorption, higher mean retention time, and enhanced area under the blood drug concentration *versus* time curve (*AUC*), indicating superior bioavailability. Furthermore, *N*-1-DNJ-Se@NVs demonstrated long-lasting hypoglycemic effect and increased cellular uptake efficiency.

Conclusion: Our findings suggest that structural derivatization improves the oral delivery of 1-DNJ and prolongs its therapeutic effect via selenized nanovesicles, positioning *N*-1-DNJ-Se@NVs as a promising nanomedicine for diabetes management.

Keywords: 1-deoxynojirimycin, nanovesicles, selenium, sustained release, hypoglycemic effect, bioavailability

Introduction

1-Deoxynojirimycin (1-DNJ), a natural compound from mulberry leaves (*Morus alba*) and certain fungi like Nocardia strains, is recognized for its hypoglycemic effects and potential to alleviate oxidative stress. Research has shown that 1-DNJ can effectively slow down glucose production and absorption by inhibiting α-glucosidase activity, thereby reducing postprandial blood glucose levels.[1,2] In addition, 1-DNJ has been found to enhance insulin sensitivity and promote glucose metabolism.[3,4] However, its rapid absorption, short half-life, and limited residence time in the body restrict its therapeutic efficacy, resulting in limited clinical application.[5–7]

Although the pharmacological activities of 1-DNJ have been well understood, formulation development remain limited. Recent advancements in oral drug delivery concentrate on enhancing oral bioavailability, stability, and therapeutic effectiveness by controlling the release of 1-DNJ. Sustained-release pellets and microspheres have been explored for this purpose.[6,8] Nano-formulations, known for their superior delivery efficiency, can improve solubility, stability, and bioavailability, rendering them a significant focus in drug development.[9,10] However, nano-drug delivery systems have not yet been applied to 1-DNJ for optimizing its bioavailability and therapy. Integrating 1-DNJ into nanocarriers is anticipated able to improve its oral bioavailability ulteriorly, thereby ameliorating its hypoglycemic effect.

Received: 10 January 2025
Accepted: 6 April 2025
Published: 10 April 2025

Directly encapsulating 1-DNJ into nanovehicles like liposomes and micelles is challenging due to its strong hydrophilicity. Introducing a hydrophobic group and further formulating it into nanovesicles may meliorate the pharmacokinetic and pharmacodynamic properties of 1-DNJ. A lipophilic group can not only increase the lipophilicity of the parent compound, but also enhance interaction with the cell membrane, thereby boosting cellular uptake. Stabilizing nanovehicles may maximize this effect by protecting them from the harsh gastrointestinal environments. In addition, selenization can reinforce the physiological stability of nanovehicles, as selenium (Se) is resistant to acid and enzymes while contributing to antioxidative and hypoglycemic benefits.[11,12] However, this combined approach has not yet been explored for constructing nanovesicles for the oral delivery of 1-DNJ.

In this study, selenized nanovesicles were engineered using the thin-film hydration method followed by in situ reduction to load *N*-oleoyl-1-DNJ (N-1DNJ). We systematically investigated the synthesis of *N*-oleoyl-1-DNJ, formulation and preparation, physiological stability, cellular uptake in Caco-2 cells, oral bioavailability, and hypoglycemic effects in Goto-Kakizaki (GK) rats. By examining these factors, we hope to develop a more effective delivery system for 1-DNJ to enhance diabetes treatment.

Materials and Methods

Materials

1-Deoxynojirimycin (1-DNJ) was procured from SAITONG Biotech Co., Ltd. (Beijing, China). Soybean lecithin was purchased from SinoPharm Chemical Reagent Co., Ltd. (Shanghai, China). DiO (3,3′-dioctadecyloxacarbocyanine perchlorate) was the product of Quansu Biotech Co., Ltd. (Beijing, China). *N, N*-diisopropylethylamine (DIPEA), O-(7-Azabenzotriazol-1-yl)-N,N,N′,N′-tetramethyluronium hexafluorophosphate (HATU), sodium selenite (Na_2SeO_3), and glutathione (GSH, reduced) were of chemical grade and from Sigma-Aldrich (Shanghai, China). Deionized water was the product of Hangzhou Wahaha Group Co., Ltd. (Hangzhou, China). HPLC-grade acetonitrile was obtained from ACMEC Biochemical (Shanghai, China). All other chemicals were of analytical grade and used as provided.

Synthesis of 1-DNJ Derivative

The acylation reaction was employed to synthesize *N*-oleoyl-1-DNJ (*N*-1-DNJ) (Figure 1).[13] Specifically, 1-DNJ, oleic acid, DIPEA, and HATU were mingled in a stoichiometric ratio of 1: 1.5: 2: 1.5 in a flask, followed by the addition of an appropriate volume of 80% acetonitrile to dissolve the reactants. The mixture was stirred for over 2 hours in ambient conditions. Liquid chromatography-mass spectrometry (LC-MS) was utilized to verify the formation of 1-DNJ derivative.

Preparation of N-1-DNJ-Se@NVs

N-1-DNJ-Se@NVs were prepared using a thin-film hydration method followed by in situ reduction.[14,15] The drug and lecithin were dissolved in methanol, which was then removed by vacuum evaporation. The resulting lipid membrane was hydrated against a 1.0 mg/mL Na_2SeO_3 solution to create vesicular dispersions. Next, the coarse vesicular dispersions were subjected to ultrasonication for homogenization of nanovesicles. After that, a four-fold molar amount of reduced GSH was added to initiate a redox reaction at 37°C for 1 h. Particle size and entrapment efficiency (*EE*) as indices were used to optimize the *N*-1-DNJ-Se@NVs formulation by varying the drug/lipid ratio, ultrasonication time, selenization time for reaction, and Na_2SeO_3 concentration.

Characterization of N-1-DNJ-Se@NVs

N-1-DNJ-Se@NVs were characterized by particle size, micromorphology, and entrapment efficiency (*EE*). The particle size was determined by dynamic light scattering using a Zetasizer Nano ZS analyzer (Malvern, Worcestershire, UK) at room temperature. Aliquots of samples (0.1 mL) were diluted with deionized water to 1.5 mL for laser diffraction. The particle size data were output with Z-average size.

The micromorphology of *N*-1-DNJ-Se@NVs was observed through transmission electron microscopy (TEM). Droplets of the nanovesicles were placed on a carbon-coated copper grid and dried using a warming lamp. The samples

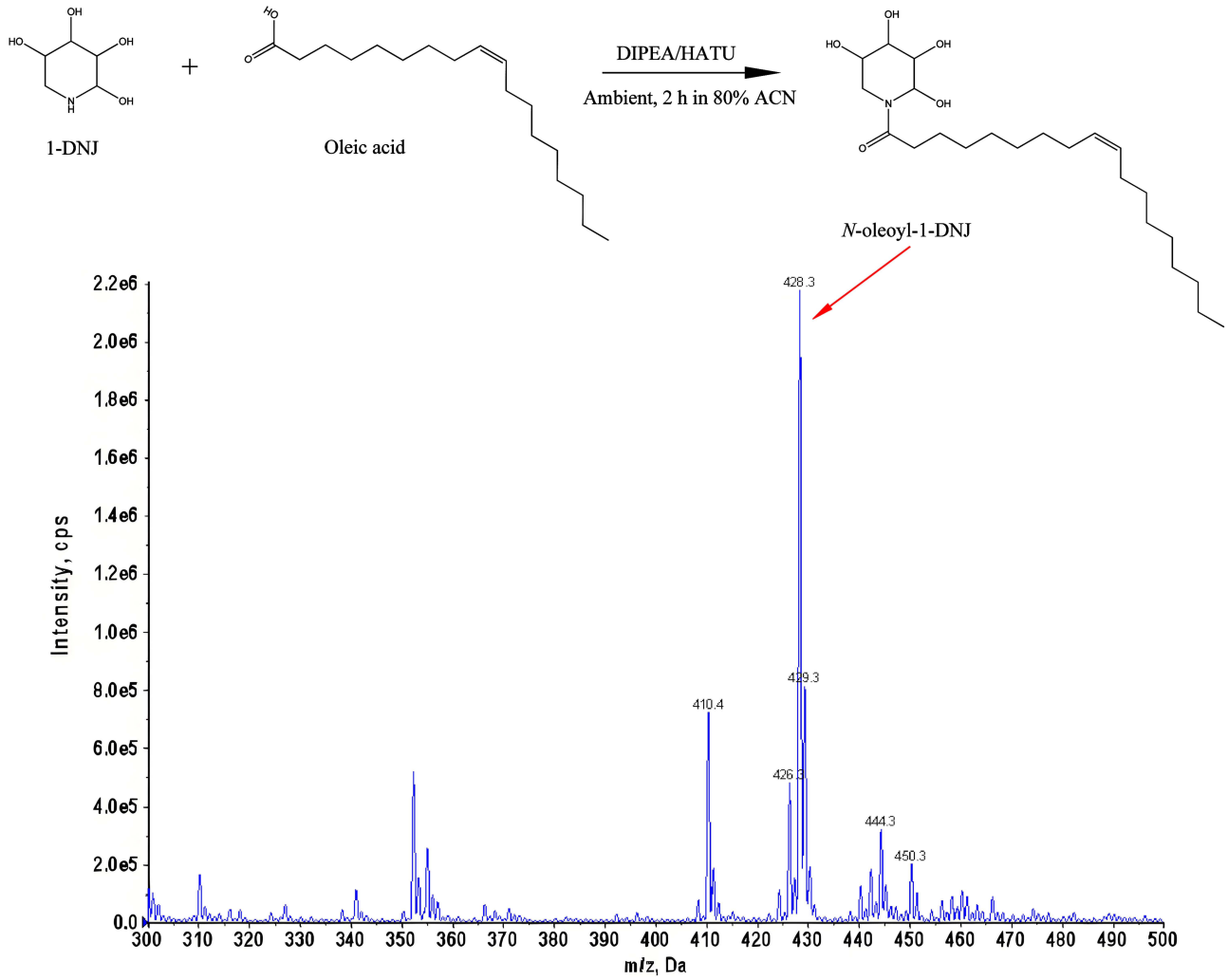

Figure 1 Synthesis and characterization of N-oleoyl-1-DNJ.

were then examined and photographed with a JEM-1400Flash TEM (JEOL, Tokyo, Japan) at an acceleration voltage of 100 kV.

The *EE* of *N*-1-DNJ-Se@NVs was measured by centrifugal ultrafiltration method.[11] Unencapsulated drug was separated from nanovesicles through sequential centrifugation and ultrafiltration with a centrifugal filter device (Amicon® Ultra-0.5, MWCO 10,000, Millipore/Merck, USA). The samples are subjected to a centrifugal force of 10,000g for 5 min. The concentrations of free drug (M_{fre}) in the filtrates and initial drug concentration in the system were quantified by UPLC. *EE* was defined as the ratio of entrapped drug (M_{ent}) to total drug (M_{tot}) and calculated using the equation of *EE* (%) = (1-M_{fre}/M_{tot}) × 100%.

Drug quantification was performed on an ACQUITY H-Class ULPC equipped with a quaternary pump, an auto-sampler, and a PDA detector (Waters, MA, USA). Samples were eluted against a BEH-C18 column (1.7 μm, 2.1 × 50 mm, Waters) at 35°C with a 3 μL injection volume. A mobile phase consisting of acetonitrile and 0.1% acetic acid solution (80/20) pumped at a flow rate of 0.2 mL/min was utilized to disunite the samples. The elution signals were monitored at 210 nm.

Stability in Simulated Gastrointestinal Fluids

The stability of nanovesicles in biorelevant media was assessed with the non-selenized formulation (*N*-1-DNJ-@NVs) as a control. The changes in particle size, PDI and ζ potential of *N*-1-DNJ-NVs and *N*-1-DNJ-Se@NVs in deionized water,

https://doi.org/10.2147/IJN.S516833

simulated gastric fluid (SGF, containing 0.32% pepsin, pH 1.2), and simulated intestinal fluid (SIF, containing 1% trypsin, pH 6.8) were investigated. Briefly, an appropriate volume of nanovesicles were mixed with water, SGF, or SIF at a 1:5 ratio and incubated at 37°C while stirring at 100 rpm. At predetermined intervals, 1 mL of sample were withdrawn for immediate analysis of particle size, PDI and ζ potential.

To explore the mechanism behind the changes in particle size, we evaluated the particle size indices by adjusting the pH of the test medium, which the nanovesicles could encounter post-administration. The same sample was divided into two parallel groups: one was directly analyzed for particle size, PDI, and ζ potential after incubation, while the other underwent neutralization with a pH conditioner before analysis.

In Vitro Release Study

The in vitro release of *N*-1-DNJ from nanovesicles was investigated in water, 0.1 M HCl, and pH 6.8 PBS with 1.2% Tween 80 as a solubilizer. Aliquots of *N*-1-DNJ-NVs or *N*-1-DNJ-Se@NVs equivalent to 5 μg of *N*-1-DNJ were dialyzed in a 100 mL release medium at 37°C using a dialysis bag with a MWCO of 10 kD. At designated time points (0.25, 0.5, 1, 2, 4, 8, 10, 12, and 24 h), 1 mL samples were withdrawn and immediately replenished with an equal volume of fresh release medium. The concentration of *N*-1-DNJ in dialyzates was analyzed, and the percentage of drug release was calculated as mean ± S.D. (n = 3).

Oral Bioavailability Study

Male GK rats weighing 200 g ± 20 g were used for the bioavailability study, with protocols approved by the Experimental Animal Ethical Committee of Jinan University (20240913–03), and the animals were conducted in strict accordance with the guidelines outlined in The Guide for the Care and Use of Laboratory Animals, published by the National Research Council (NRC). The rats were randomly divided into 3 groups (n = 5) and fasted for 12 hours with access to water *ad libitum*. Then, *N*-1-DNJ suspensions, *N*-1-DNJ-NVs, and *N*-1-DNJ-Se@NVs were administered by gavage at a dose of 30 mg/kg with reference to the previous literature,[3,16] respectively. Blood samples (approximately 0.25 mL) were collected into heparinized centrifuge tubes from the tail vein at 0.25, 0.5, 1, 2, 4, 6, 8, 12, and 24 h post-administration. After mixing, the upper plasma layer was collected following centrifugation at 5000 rpm for 10 minutes. *N*-1-DNJ was extracted from the plasma and quantified by UPLC-MS as described below. The blood drug concentration over time was plotted, and pharmacokinetic parameters were analyzed using DAS 2.0 software.

Samples for UPLC-MS analysis were prepared by liquid-liquid extraction. In 100 μL of plasma, 200 μL of ethyl acetate were added along with 10 μL of fenofibrate (100 μg/mL) as an internal standard. After centrifugation at 10,000 rpm for 10 minutes, the upper ethyl acetate layer was separated, and an additional 200 μL of ethyl acetate was added for a second extraction. The two extraction solutions were combined and dried at 45°C in a vacuum centrifuge for 30 minutes. The residues were reconstituted in 500 μL of methanol for UPLC-MS analysis. Drug analysis was conducted on a SCIEX Triple Quad LC-MS/MS system (AB SCIEX, MA, USA) using an ACQUITY BEH-C18 column (1.7 μm, 2.1 × 50 mm, Waters) at 35°C with a 5 μL injection. Gradient elution was performed with 1% formic acid aqueous solution as mobile phase A and acetonitrile as mobile phase B at a flow rate of 0.3 mL/min. The gradient program was 5% B from 0 to 3 min, 5% to 90% B from 3 to 7 min, 90% B from 7 to 9 min, and 5% B from 9 to 12 min. The mass spectrometry settings included Turbo Spray ion source, positive ion detection mode, multiple reaction monitoring (MRM), ion source temperature (TEM) at 500°C, curtain gas (CUR) at 30 psi, ion spray voltage (IS) at 4500 V, and ion source gas (GS) at 30 psi.

Hypoglycemic Effect in Diabetic Rats

Adult GK rats (250 ± 20 g), a well-established model of type 2 diabetes,[17] were used to investigate the hypoglycemic effects of *N*-1-DNJ-Se@NVs and reference formulations. Male GK rats were randomly divided into four groups (n = 5): control, *N*-1-DNJ suspension, *N*-1-DNJ-NVs, and *N*-1-DNJ-Se@NVs. The rats were fasted overnight but allowed free access to water. They received the above-mentioned formulations containing sucrose (3.6 mg/mL) at a dose of 30 mg/kg by gavage. Blood glucose levels were measured at 0.25, 0.5, 1, 2, 4, 6, 8, 12, and 24 h using a glucose assay kit (Jiancheng Bioengineering Institute, Nanjing, China). Blood glucose concentration was calculated with the equation:

Blood glucose (mM) = $(A_s\text{-}A_b)/(A_c\text{-}A_b) \times 5.05$, where A_s, A_b and A_c represent the absorbance of the test, blank, and calibration samples, respectively, with 5.05 being the glucose concentration of the calibration solution.[18]

Cellular Uptake and Internalization

Cell uptake of *N*-1-DNJ-NVs and *N*-1-DNJ-Se@NVs was analyzed using flow cytometry. Caco-2 cells, obtained from the American Type Culture Collection (ATCC), were procured through BDBIO Biotechnology Co., Ltd and cultured in 6-well plates for over 24 hours at a density of 5×10^5 cells per well. DiO-labeled N-1-DNJ-NVs and N-1-DNJ-Se@NVs were freshly prepared by dissolving the agent into the organic phase, following the same procedure as unlabeled nanovesicles. Fluorescent *N*-1-DNJ-NVs and *N*-1-DNJ-Se@NVs were incubated with Caco-2 cells at a concentration of 10 μg/mL *N*-1-DNJ at 37°C for 0.5, 1, and 2 h, respectively. Fluorescence intensity was measured by flow cytometry, and the cell uptake rate was calculated based on the positive cell count.

Cellular internalization of nanovesicles was observed by confocal laser scanning microscopy (CLSM). Caco-2 cells were grown in confocal petri dishes at a density of 1×10^5 cells per well for 24 h, with the dishes pre-balanced with medium. DiO-labeled nanovesicles were then added and incubated for 1 hour. After incubation, the cells were fixed in 4% paraformaldehyde at 4°C for 30 minutes, followed by nuclear staining with Hoechst 33258. Finally, internalization was observed and photographed under CLSM.

To explore cellular trafficking mechanisms, the uptake of nanovesicles was analyzed with inhibitors (sucrose, chlorpromazine, simvastatin, and genistein) or under low temperature. Caco-2 cells were cultured in 6-well plates for over 24 hours. Once attached, the culture medium was removed, and 1 mL of fresh medium loading an appropriate concentration of inhibitors was added for another 30 minutes of incubation. Subsequently, DiO-labeled *N*-1-DNJ-NVs or *N*-1-DNJ-Se@NVs were added and incubated for 2 hours. Additionally, cellular uptake at 4°C was assessed to investigate the effect of temperature. All measurements were conducted with a flow cytometer (FACSCanto, BD, New York, USA), and the cellular trafficking pathways of nanovesicles were elucidated based on relative uptake under these conditions.

Cytotoxicity Test

The cytotoxicity of *N*-1-DNJ, *N*-1-DNJ-NVs and *N*-1-DNJ-Se@NVs was assessed using the MTT assay. Caco-2 cells were cultured in DMEM supplemented with 20% fetal bovine serum and 1% penicillin-streptomycin at 37°C in a 5% CO_2 incubator. The cells were seeded in 96-well plates at a density of 1×10^4 cells per well and cultured for 24 h. The preparations were diluted into 7 levels using culture medium and incubated with the cells for 6 h, 12 h and 24 h, respectively. MTT solution and DMSO were then added in sequence. After the purple crystals dissolved completely, the optical density (OD) at 490 nm was measured using a microplate reader to calculate relative cell activity.

Results and Discussion

Synthesis of N-Oleoyl-1-DNJ

Amines and organic acids can be readily acylated with activating and condensing agents. In this experiment, DIPEA activated oleic acid, which then combined with HATU to complete the acylation with 1-DNJ. LC-MS confirmed the successful condensation between 1-DNJ and oleic acid, with the product's molecular mass measured at 427, corresponding to the combined masses of the two reactants (163 and 282) after acylation (Figure 1). The introduction of the oleic acid group enhanced the lipophilicity of 1-DNJ, facilitating its encapsulation into nanovesicles.

Preparation and Characterization of N-1-DNJ-Se@NVs

Thin-film hydration represents a well-established method for preparing vesicles.[19] During hydration, the lipid membrane curls, sealing the water phase to form lipid vesicles. In our study, we employed this approach to prepare lipid vesicles and fabricated selenized nanovesicles via in situ reduction technique. The effects of formulation and preparative variables on properties of vesicles are shown in Figure 2. The drug/lipid ratio significantly influenced vesicle size but had little effect on *EE*. A 1:4 drug/lipid ratio produced smaller vesicles with higher EE, so this ratio was fixed for subsequent

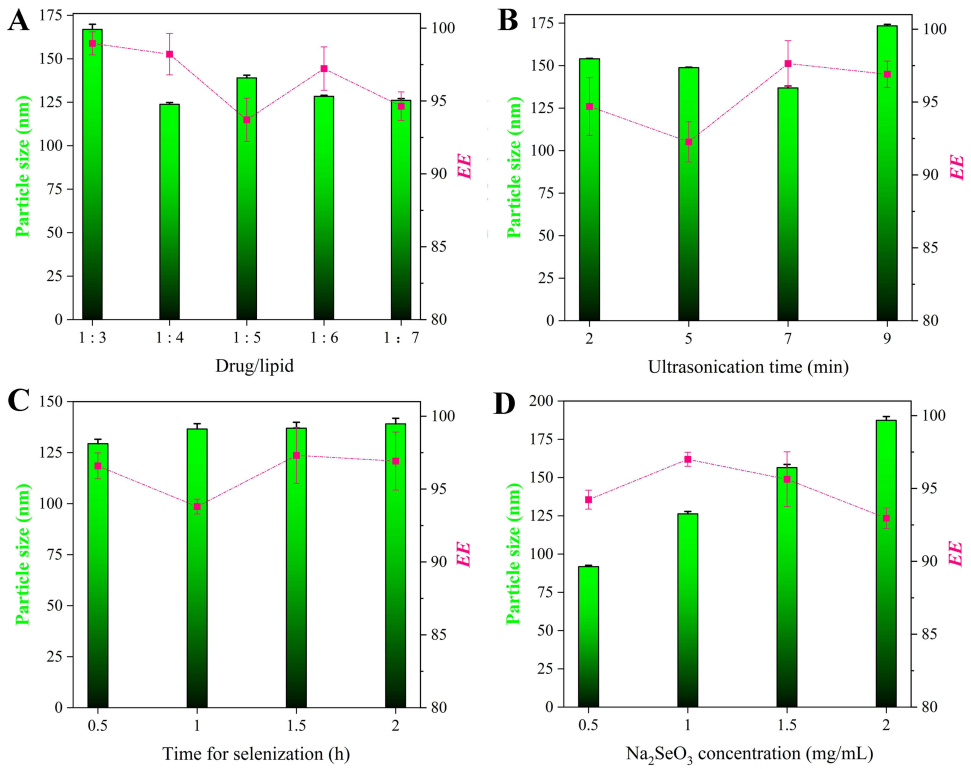

Figure 2 The effects of formulation variables on particle size, polydispersity index (PDI) and entrapment efficiency (*EE*) of nanovesicles, including drug/lipid ratio (**A**), ultrasonication homogenization time (**B**), selenization reaction time (**C**), and Na_2SeO_3 concentration upon in situ reduction (**D**). All experiments were performed in triplicate.

experiments. Prior to selenization, vesicles should be homogenized for uniformity, with ultrasonication being crucial for achieving eligible nanovesicles. The ultrasonic time has a great influence on the particle size of vesicles. Ultrasonication time greatly affected vesicle size that sonication for 7 minutes yielded the smallest vesicles and highest *EE*. Particle size changes indicate the completion of the selenization reaction. The smallest vesicles were obtained at 0.5 h after selenization. After 1 h, the vesicle size stabilized, confirming that this time was optimal for reaction. In addition, the size of nanovesicles increased with incremental concentration of Na_2SeO_3, with 1.0 mg/mL being ideal, resulting in vesicle sizes below 150 nm. Overall, formulation and preparative factors had marginal impact on *EE*, which remained above 90%, suggesting that oleoylation effectively enhances the encapsulation of 1-DNJ. It is believed to be beneficial for bioavailability and effect enhancement.

Taken together, the formulation of *N*-1-DNJ-Se@NVs was finalized with a drug/lipid ratio of 1:4, ultrasonication for 7 min, selenization for 1 h, and a Na_2SeO_3 concentration of 1.0 mg/mL. The preferred formulation resulted in translucent orange-red *N*-1-DNJ-Se@NVs (Figure 3A), distinct from the colorless *N*-1-DNJ-NVs. The particle size was measured to be 115.4 nm with a PDI of 0.161 (Figure 3B), larger than that of *N*-1-DNJ-NVs. The ζ potential of *N*-1-DNJ-Se@NVs was −41.2 mv, higher than that of *N*-1-DNJ-NVs, showing good colloidal stability.[20] The morphology of *N*-1-DNJ-Se @NVs were spherical as revealed by TEM (Figure 3C). There were significant differences in appearance, particle size, and ζ potential between *N*-1-DNJ-NVs and *N*-1-DNJ-Se@NVs, aside from *EE*. These differences confirm successful Se deposition onto vesicles after in situ reduction.

Improved Physiological Stability of Nanovesicles via Selenization

The in vivo behavior of nanocarriers is closely linked to their absorption and drug delivery effectiveness. Lipid formulations are reported to be easily disrupted in digestive media.[18] Generally, the physiological stability of nanovesicles can be indicated by particle size, PDI, and ζ potential. In this study, biorelevant media, including deionized water, SGF, and SIF, were utilized to assess the GI stability of *N*-1-DNJ-Se@NVs. Figure 4 illustrates the changes in particle

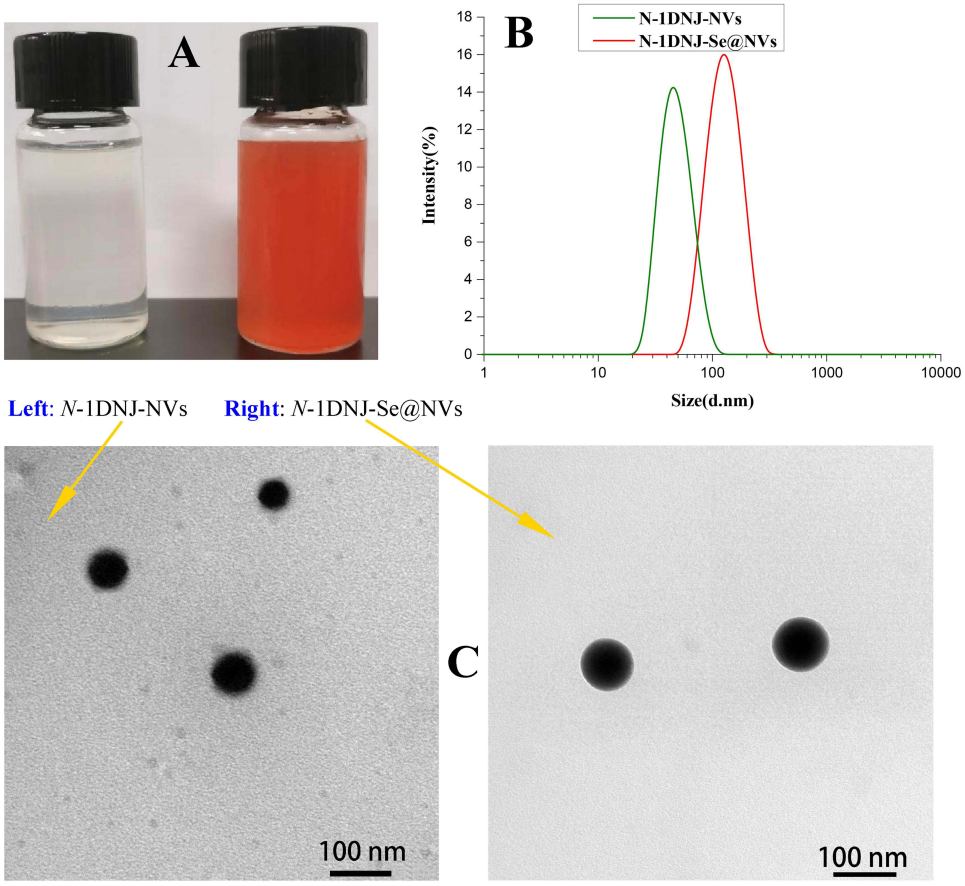

Figure 3 Comparable properties between N-1-DNJ-NVs and N-1-DNJ-Se@NVs: (**A**) appearance, (**B**) particle size distribution, and (**C**) micromorphology.

size, PDI, and ζ potential of nanovesicles over time when incubated with these fluids. The nanovesicles remained stable in deionized water and SIF, showing no significant changes in size, PDI, or ζ potential (Figure 4A). In contrast, significant alterations were observed in SGF, where particle size increased, PDI fluctuated, and interfacial charge reversed, particularly for N-1-DNJ-NVs. In order to elucidate the underlying mechanism, we neutralized the SGF-incubated samples to pH 7.4 with NaOH and re-evaluated the parameters. Notably, after neutralization, the particle size, PDI, and ζ potential of both nanovesicles nearly returned to their initial state (Figure 4B). These results suggest that the nanovesicles were not digested or degraded in the harsh gastric environment but were instead protonated. Both *N*-1-DNJ-NVs and *N*-1-DNJ-Se@NVs were negatively charged, leading to protonation in the acidic conditions. Protonation tends to cause aggregation of particles, fluctuation of PDI, and reversal of interfacial charge.[21] Of note, *N*-1-DNJ-Se@NVs demonstrated greater resistance to acid protonation than *N*-1-DNJ-NVs due to the surface Se deposition.

In Vitro Drug Release

The release profiles of *N*-1-DNJ from nanovesicles in various media are illustrated Figure 5. Overall, free *N*-1-DNJ exhibited the fastest release rate, followed by *N*-1-DNJ-NVs, and then *N*-1-DNJ-Se@NVs. In deionized water, 0.1M HCl, and pH 6.8 PBS, the accumulative release of *N*-1-DNJ from the solution formulation was 86.64%, 85.08%, and 92.42%, respectively, within 24 hours. In comparison, *N*-1-DNJ-NVs released 79.43%, 64.40%, and 82.85%, and *N*-1-DNJ-Se@NVs released approximately 72.36%, 64.22%, and 75.19%. These results indicate that *N*-1-DNJ-Se @NVs offer a more sustained release due to Se coting. The incomplete release of free drug can be attributed to the dialysis bag's resistance, while the slow release for vesicular formulations in 0.1 M HCl is linked to vesicle surface protonation, since protonation can condense nanovesicles whereby to sustain drug release, aligning with the findings of stability study. The reduced release suggests that a thin Se layer was formed on the nanovesicle's surface through in situ

https://doi.org/10.2147/IJN.S516833

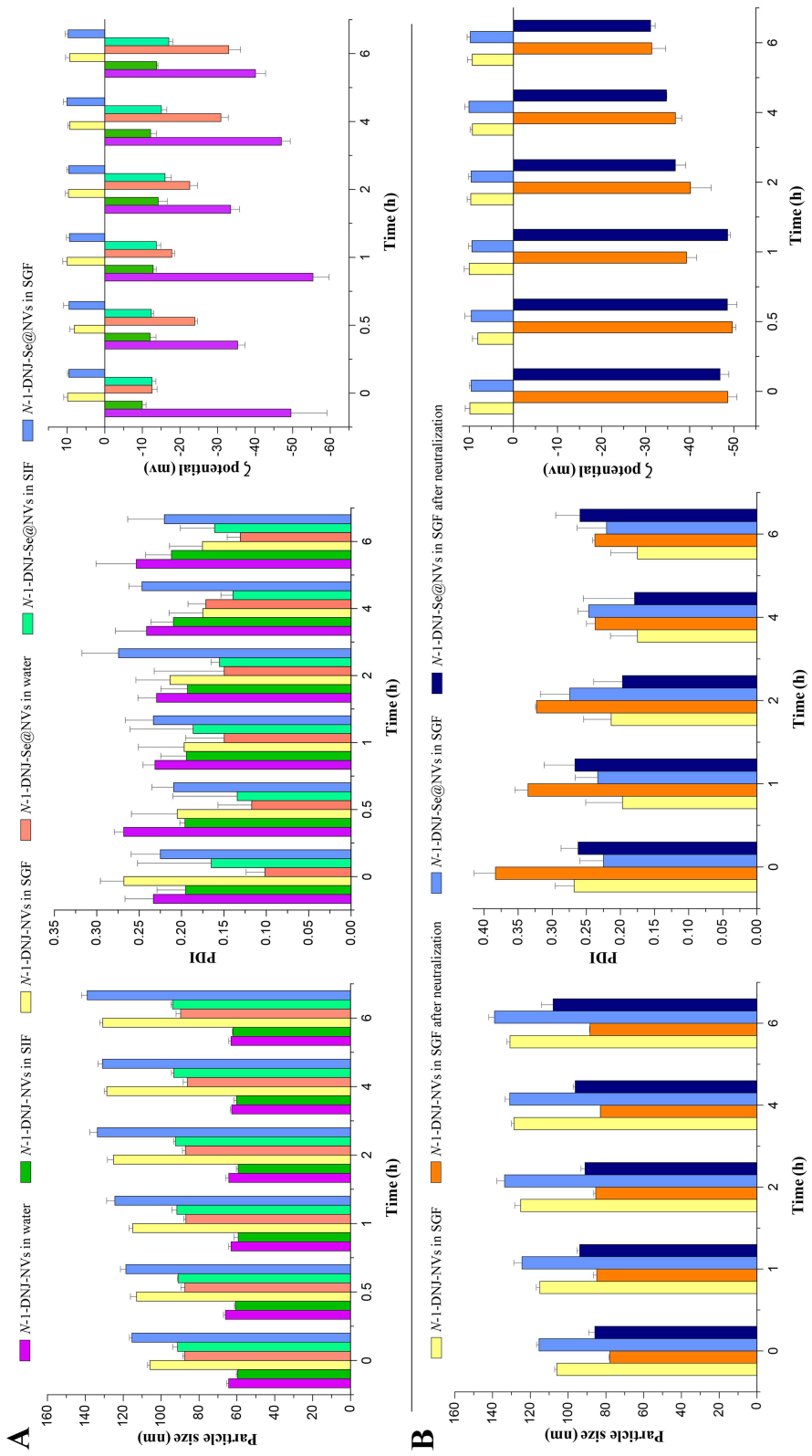

Figure 4 Physiological stability of *N*-1-DNJ-NVs and *N*-1-DNJ-Se@NVs in simulated gastrointestinal fluids: (**A**) changes in particle size, PDI and ζ potential over time as incubated with deionized water, SIF, and SGF; (**B**) changes in particle size, PDI and ζ potential over time in SGF with or without NaOH neutralization (n = 3, mean ± SD).

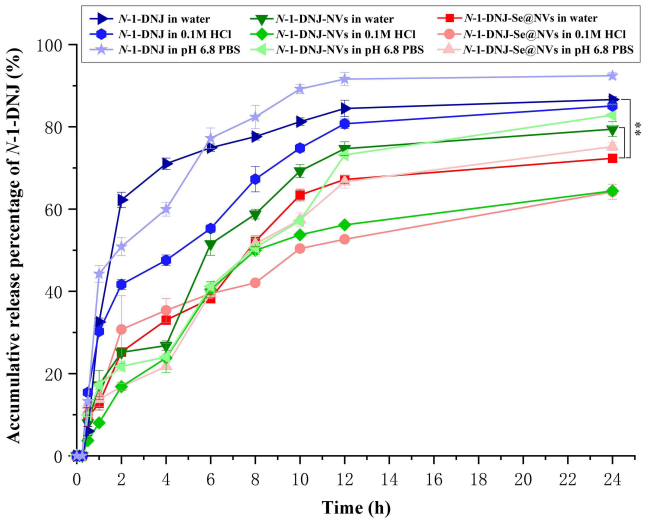

Figure 5 In vitro release profiles of *N*-1-DNJ from nanovesicles in deionized water, pH 1.2 hCl, and pH 6.8 PBS. Data expressed as mean ± SD ($n = 3$), paired *t*-test, ** $P < 0.01$, significantly different between two groups.

reduction. pH-dependent drug release minimizes premature release of the active ingredient in the stomach, which facilitates its intestinal absorption through integral nanovesicles, hence the oral bioavailability enhancement.

Enhanced Oral Bioavailability

After administration of *N*-1-DNJ suspensions, *N*-1DNJ-NVs, and *N*-1DNJ-Se@NVs to GK rats, the blood concentration versus time curves are displayed in Figure 6, with basic pharmacokinetic parameters from the one-compartmental model summarized in Table 1. *N*-1-DNJ suspensions group exhibited faster drug absorption, likely due to the enhancive lipophilicity from oleoylation. However, while the blood concentration rose quickly, it also declined rapidly for unencapsulated drug, indicating a short in vivo residence time and limited long-term therapeutic effect. In contrast, the *N*-1DNJ-NVs and *N*-1DNJ-Se@NVs groups showed retardant absorption but significantly improved extent and prolonged residence time, which will be beneficial for prolonging its curative effect. The maximum plasma concentration (C_{max}) decreased in both groups, but the peak time to C_{max} (T_{max}) for both groups was notably lagged, increasing from 3.08 hours to 6.64 and 9.17 hours, respectively. Correspondingly, the mean retention time (*MRT*) increased

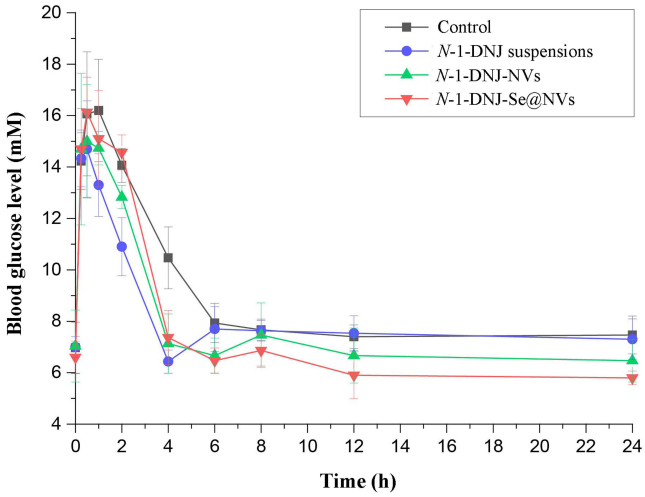

Figure 6 Plasma drug concentration versus time profiles of *N*-1-DNJ suspensions, *N*-1-DNJ-NVs, and N-1-DNJ-Se@NVs in GK rats following oral administration at a dose of 30 mg/kg (mean ± SD, $n = 5$).

https://doi.org/10.2147/IJN.S516833

Table 1 Pharmacokinetic Parameters Derived From One-Compartmental Model After Oral Administration of N-1-DNJ Suspensions, N-1-DNJ-NVs, and N-1-DNJ-Se@NVs in GK Rats

PK Parameter	*N*-1-DNJ Suspensions	*N*-1-DNJ-NVs	*N*-1-DNJ-Se@NVs
C_{max} (ng/mL)	127.29 ± 16.43	105.75 ± 25.52	105.18 ± 10.97
T_{max} (h)	3.08 ± 1.28	6.64 ± 1.16*	9.17 ± 1.25$^{\#}$
$AUC_{0-\infty}$ (ng/mL*h)	1065.82 ± 72.58	1671.67 ± 323.66**	1909.84 ± 234.92$^{\#}$
$t_{1/2}$ (h)	2.19 ± 0.15	4.84 ± 1.063**	6.66 ± 1.20$^{\#}$
$MRT_{0-\infty}$ (h)	6.16 ± 0.984	13.29 ± 2.16**	18.37 ± 1.57$^{\#\#}$

Notes: statistical, ANOVA, *$p < 0.05$, **$p < 0.01$, compared with *N*-1-DNJ suspensions; $^{\#}p < 0.05$, $^{\#\#}p < 0.01$, compared with *N*-1-DNJ-NVs.

approximately 2.16 times for *N*-1DNJ-NVs and 2.98 times for *N*-1DNJ-Se@NVs. Additionally, the area under the blood concentration-time curve (*AUC*) for *N*-1DNJ-Se@NVs group was the highest, up to 1.79 times that of the suspensions and 1.57 times that of the N-1DNJ-NVs group, indicating that selenized nanovesicles could slowly and persistently promote the absorption of *N*-1-DNJ molecules. The half-life ($t_{1/2}$) for the *N*-1DNJ-Se@NVs group was 8.04 hours longer than that of the suspension and *N*-1DNJ-Se@NVs, suggesting restrictive drug metabolism. Even at the last sampling, the plasma drug concentration in the *N*-1DNJ-Se@NVs group remained higher than in the other two groups, reflecting an optimal absorption profile. Overall, *N*-1DNJ-Se@NVs demonstrated greater absorption extent and longer action time compared to free drug and non-selenized nanovesicles.

1-DNJ can effectively inhibits the activity of α-glucosidase, thus reducing postprandial blood glucose levels in humans. However, its rapid absorption limits its pharmacological effect compared to other α-glucosidase inhibitors. To solve the absorption challenge, researchers have employed sustained-release materials to improve the oral delivery of this phytomedicine. Wang et al utilized carboxymethylcellulose sodium (CMC-Na) to facilitate oral delivery of 1-DNJ, demonstrating that CMC-Na can suppress and delay absorption and remarkably improve the activity of 1-DNJ on glucose levels.[22] Similarly, Sun et al developed sustained-release pellets that enhanced the relative bioavailability of 1-DNJ to 117.3% compared to immediate-release tablets, showcasing a promising formulation strategy.[8] Our study aims to optimize the pharmacokinetic properties of 1-DNJ through derivatization and combined formulation strategy. The results indicate that structural derivatization extended the in vivo half-life and residence time of 1-DNJ, while selenized nanovesicles further improved its bioavailability by delaying absorption. This approach offers a solution for maintaining the long-lasting efficacy of 1-DNJ in diabetes management.

Ameliorative Hypoglycemic Effects Through N-1-DNJ-Se@NVs

The hypoglycemic effects of *N*-1-DNJ suspensions, *N*-1DNJ-NVs, and *N*-1DNJ-Se@NVs in GK rats were assessed by monitoring blood glucose levels after administration. As shown in Figure 7, all groups exhibited high blood glucose level from 0.25 to 2 h, likely due to stress during administration, a phenomenon noted in other studies.[23–25] Mechanically, 1-DNJ reduces glucose generation and absorption by inhibiting carbohydrate breakdown, thereby slowing the rise in postprandial blood glucose.[3] Blood glucose levels in the treatment groups were lower than in the control group. At 4 h, the suspension group reached the lowest blood glucose level of 6.4 ± 0.4 mm, consistent with the pharmacokinetic findings. The other treatment groups also showed significant decreases in blood glucose, while the control group remained the highest. From 6 h to 24 h, blood glucose levels in both the control and suspension groups stabilized between 7.0 and 7.7 mm, indicating the suspension group's pharmacological effect had diminished. In contrast, the N-1DNJ-NVs and N-1DNJ-Se@NVs groups' blood glucose continued to decline slowly at 6 hour, slightly increased at 8 hour, then decreased again from 12 to 24 hour, stabilizing afterward. The final blood glucose levels measured were 6.5 ± 0.83 mm and 6.1 ± 0.56 mm, respectively, approaching a normal level. Overall, the blood glucose curves for *N*-1DNJ-NVs and *N*-1DNJ-Se@NVs groups were similar, though the *N*-1DNJ-Se@NVs group showed slightly lower levels after 8 h due to its sustained-release effect, resulting in a more lasting hypoglycemic effect.

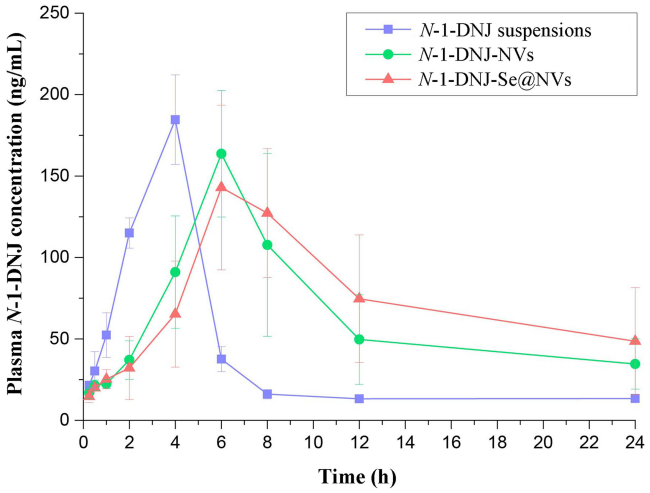

Figure 7 Blood glucose concentration versus time curves of *N*-1-DNJ suspensions, *N*-1-DNJ-NVs, and N-1-DNJ-Se@NVs in GK rats after oral administration at a dose of 30 mg/kg (mean ± SD, *n* = 5).

1-DNJ primarily inhibits glycosidases like sucrase, maltase, α-glucosidase, and α-amylase, preventing the breakdown of saccharides into glucose and thereby curbing blood glucose rise-up at the absorption level.[26] Rapid absorption of 1-DNJ as well as its derivatives is disadvantageous to the inhibition of carbohydrate breakdown, even though 1-DNJ can improve insulin resistance via the PI3K/AKT signaling pathway.[27,28] On the contrary, slow and steady absorption will enhance the glucose-controlling effect of such glucosidases. In this study, to precisely investigate the glycemic regulation effect of *N*-1-DNJ, sucrose was intentionally added into preparations during administration. To achieve effective and continuable blood glucose control, *N*-1-DNJ must be remained in the body long enough to inhibit carbohydrate breakdown during absorption and alleviate insulin resistance in circulation. The antioxidant activity of 1-DNJ contributes to mitigation of insulin resistance.[29] Se is a well-known antioxidant that helps to mitigate oxidative stress, a key contributor to insulin resistance and β-cell dysfunction in diabetes.[30] The combination of 1-DNJ and Se demonstrates a synergistic potential to enhance the PI3K/AKT signaling pathway, improve β-cell function, and attenuate inflammation. This synergistic effect may be attributed to the complementary mechanisms of α-glucosidase inhibition by 1-DNJ, enhanced insulin signaling through the PI3K/AKT pathway, and the antioxidant and anti-inflammatory properties of Se.[31,32] Together, these multi-faceted actions contribute to improved glycemic control and reduced insulin resistance. Furthermore, our engineered nano-drug delivery system amplifies the pharmacological efficacy of this combination by prolonging the residence of active ingredients in the gut, promoting their absorption into systemic circulation, and enabling sustained blood glucose regulation. This innovative approach ensures optimal therapeutic outcomes by maximizing the bioavailability and synergistic effects of 1-DNJ and Se.

Cellular Uptake and Trafficking Patterns

Figure 8 displays the cellular uptake of two types of vesicular *N*-1-DNJ in Caco-2 cells, as analyzed by flow cytometry. The uptake increased over time, with *N*-1-DNJ-Se@NVs slightly higher uptake than *N*-1-DNJ-NVs. At 0.5 h, 1 h, and 2 h, the uptake rates for *N*-1-DNJ-NVs were 31.67%, 59.47%, and 74.63%, respectively, while *N*-1-DNJ-Se@NVs had rates of 46.93%, 68.67%, and 81.5%. Overall, *N*-1-DNJ-Se@NVs exhibited uptake rates 6.9% to 15.3% higher than *N*-1-DNJ-NVs, likely due to non-specific endocytosis of selenized nanovesicles by cells. The results indicate that selenization promotes the cellular uptake of vesicles to some extent without negatively impacting the uptake.

CLSM imaging revealed the cellular internalization of the two nanovesicles. The intensity of green fluorescence indicates the degree of internalization, with DiO-labeled vesicles fluorescing green and Hoechst-stained nuclei fluorescing blue. The imaging clearly shows that the *N*-1-DNJ-Se@NVs and *N*-1-DNJ-NVs-associated fluorescence diffuses throughout the whole cell colony. In contrast, *N*-1-DNJ-Se@NVs exhibit brighter fluorescence, suggesting that selenized vesicles have meliorative cellular uptake, potentially contributing to absorption enhancement. Anyway, Se layering does not affect the cellular uptake of nanovesicles, except to delay drug release.

https://doi.org/10.2147/IJN.S516833

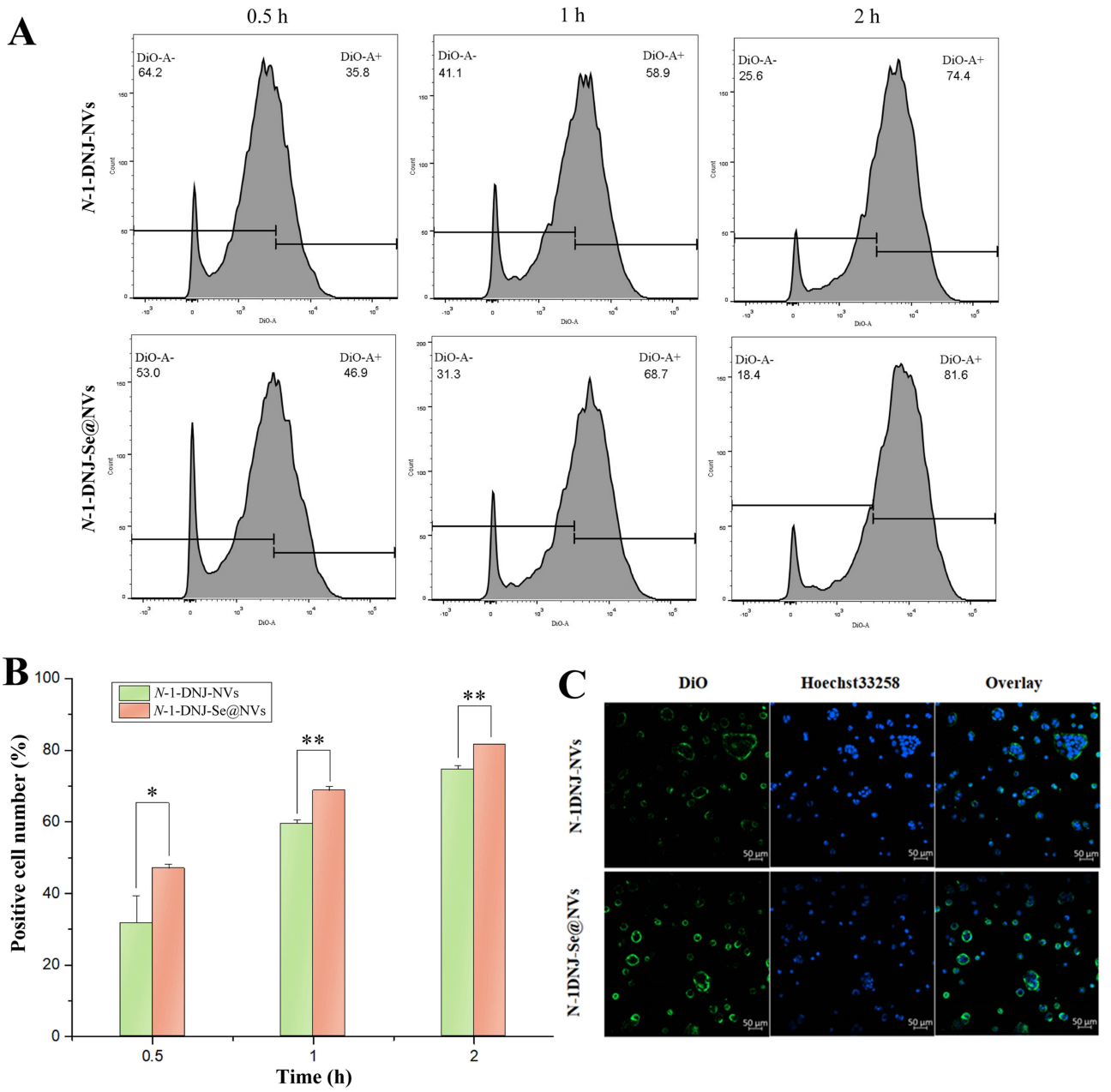

Figure 8 Cellular uptake and internalization of *N*-1-DNJ-NVs and *N*-1-DNJ-Se@NVs in Caco-2 cells. A. cytometric diagrams of positive cells stained by DiO-labeled nanovesicles after incubation for 0.5, 1, and 2 h, respectively; (**B**) histograms of positive cell number; and (**C**) CLSM imaging for internalized nanovesicles. Data expressed as mean ± SD ($n = 3$), paired t-test, *$p < 0.05$, **$p < 0.01$, significantly different between two groups.

The effect of transport inhibitors on the uptake of nanovesicles is shown in Figure 9. Apart from chlorpromazine, hypertonic sucrose, simvastatin, and genistein inhibited the uptake of both *N*-1-DNJ-NVs and *N*-1-DNJ-Se@NVs, with a lesser inhibition on N-1-DNJ-Se@NVs. When compared to chlorpromazine, other inhibitors reduced cell uptake by 16.1%-24.44% for *N*-1-DNJ-NVs and 13.07%-17.57% for *N*-1-DNJ-Se@NVs. Moreover, uptake inhibition was particularly pronounced at 4°C, leading to over 90% reduction, likely due to increased membrane rigidity, which blocks energy-dependent uptake and passive diffusion.[33] The results indicate that non-specific clathrin- and caveolin-mediated endocytosis is involved in the uptake of both *N*-1-DNJ-NVs and *N*-1-DNJ-Se@NVs. Hypertonic sucrose and chlorpromazine inhibit non-specific and specific clathrin-mediated endocytosis, while simvastatin and genistein inhibit non-specific and specific caveolin-

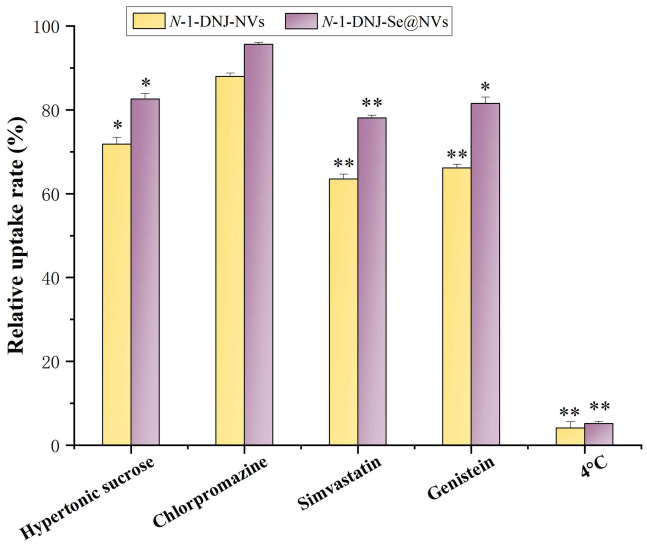

Figure 9 Cellular trafficking pathways study with Caco-2 cells analyzed through the relative uptake in the presence of physiological inhibitors or under 4°C compared with control. Data expressed as mean ± SD (n = 3, paired-t test, *p < 0.05; **p < 0.01, significantly different compared with the control).

mediated endocytosis, respectively.[34] *N*-1-DNJ-NVs are significantly affected by specific caveolin-mediated endocytosis, whereas *N*-1-DNJ-Se@NVs are less impacted, suggesting that they utilize different trafficking pathways.[11,35]

Cytotoxicity

The cytotoxicity of *N*-1-DNJ in solution against Caco-2 cells was evaluated using the MTT assay at concentrations ranging from 0.5 to 15 μg/mL over 6, 12, and 24 h. At concentrations between 0.5 and 10 μg/mL, the cell survival rate remained above 80% across all time points (Figure 10). However, cytotoxicity was observed at a higher concentration, indicating a concentration-dependent effect. To further explore the influence of formulation, we evaluated the cytotoxicity of *N*-1-DNJ-NVs and *N*-1-DNJ-Se@NVs, both containing 10 μg/mL of N-1-DNJ. After 24 hours of incubation, the cell viability decreased to 39.79% and 72.79% for *N*-1-DNJ-NVs and *N*-1-DNJ-Se@NVs, respectively, significantly lower than the control (free *N*-1-DNJ) at the same concentration. The enhancive cytotoxicity is attributed to increased cellular uptake mediated by the nanovesicles, resulting in elevated intracellular *N*-1-DNJ concentrations and increased cell death. Importantly, this increase in cytotoxicity is not caused by the carrier but rather the result of improved drug uptake by the cells.

It is difficult to reach concentrations as high as 10 μg/mL for N-1-DNJ in vivo after administration. Oral pharmacokinetic studies have revealed a maximum circulating blood concentration of only 0.127 μg/mL, significantly lower than the minimum toxic concentration observed in vitro. Therefore, there is no need to worry about the damage to the

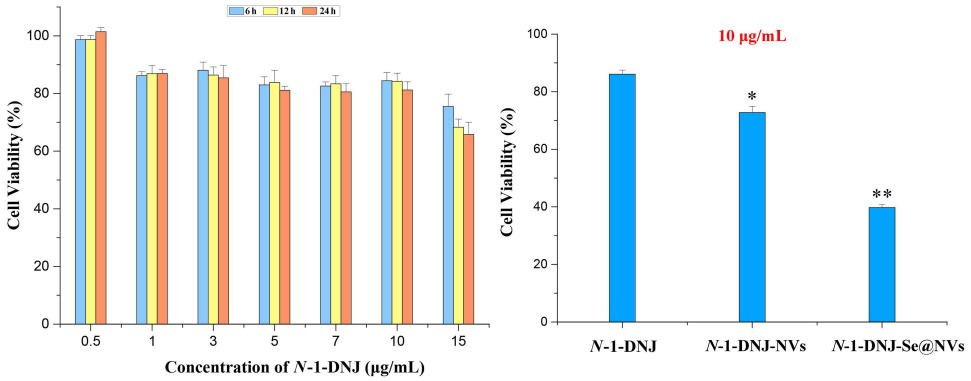

Figure 10 Cytotoxicity of *N*-1-DNJ, *N*-1-DNJ-NVs and *N*-1-DNJ-Se@NVs tested with Caco-2 cells. Paired-t test, *p < 0.05; **p < 0.01 (n = 3), significantly different compared with *N*-1-DNJ.

https://doi.org/10.2147/IJN.S516833

gastrointestinal tract and other body tissues with the use of *N*-1-DNJ-loaded nanovesicles. The exclusive benefit of selenized nanovesicles lies in their potential to increase drug residence time and prolong therapeutic effect. While this work has made progress in improving the pharmacokinetic properties of 1-DNJ, several limitations warrant consideration. The research is confined to the GK rat model, lacking validation data in other diabetic animal models. The nanoformulation's long-term safety profile remains to be conducted. Furthermore, the precise molecular mechanisms underlying the observed therapeutic effects also require further elucidation.

Conclusions

This study successfully synthesized *N*-oleoyl-1-DNJ and developed a Se-decorated nanovesicular formulation, offering significant advantages in drug delivery and therapy. The nanovesicles, prepared by the thin-film hydration/in situ reduction technique, demonstrated better physiological stability than non-selenized versions, particularly in gastrointestinal environments, with enhanced stability and sustained release. Pharmacokinetic studies demonstrated that *N*-1-DNJ-Se@NVs had superior absorption and longer duration in GK rats compared to free drug and non-selenized nanovesicles, underscoring their potential to improve oral bioavailability. Additionally, *N*-1-DNJ-Se@NVs exhibited more sustained effects on lowering blood glucose levels, indicating promising applications in diabetes treatment. Cellular uptake experiments revealed that selenization enhanced the efficiency of cellular uptake while maintaining acceptable cytotoxicity levels. *N*-1-DNJ-Se@NVs represent a novel nano drug carrier with the potential to prolong drug action and enhance therapeutic effects. However, further research is required to elucidate the molecular mechanisms on antidiabetic action, optimize targeted delivery, and explore the synergistic interaction between *N*-1-DNJ and selenium at the molecular level for clinical translation.

Acknowledgments

This work was supported by the Guangdong Basic and Applied Basic Research Foundation (2023A1515012326), the Major Projects Supported by Anhui Provincial Department of Education for Outstanding Young Talents of Universities (gxyqZD2022104), and the Research Project of Guangdong Provincial Bureau of Traditional Chinese Medicine (20262026 and 20241319).

Disclosure

The authors report no conflicts of interest in this work.

References

1. Thakur K, Zhang -Y-Y, Mocan A. et al. 1-Deoxynojirimycin, its potential for management of non-communicable metabolic diseases. *Trends Food Sci Technol*. 2019;89:88–99. doi:10.1016/j.tifs.2019.05.010
2. Kim JY, Ok HM, Kim J, et al. Mulberry leaf extract improves postprandial glucose response in prediabetic subjects: a randomized, double-blind placebo-controlled trial. *J Med Food*. 2015;18(3):306–313. doi:10.1089/jmf.2014.3160
3. Li Y-G, Ji D-F, Zhong S, et al. 1-deoxynojirimycin inhibits glucose absorption and accelerates glucose metabolism in streptozotocin-induced diabetic mice. *Sci Rep*. 2013;3(1):1377. doi:10.1038/srep01377
4. Ren X, Xing Y, He L, et al. Effect of 1-Deoxynojirimycin on insulin resistance in prediabetic mice based on next-generation sequencing and intestinal microbiota study. *J Ethnopharmacol*. 2022;289:115029. doi:10.1016/j.jep.2022.115029
5. Nakagawa K, Kubota H, Kimura T, et al. Occurrence of orally administered mulberry 1-deoxynojirimycin in rat plasma. *J Agric Food Chem*. 2007;55(22):8928–8933. doi:10.1021/jf071559m
6. Vichasilp C, Nakagawa K, Sookwong P, et al. A novel gelatin crosslinking method retards release of mulberry 1-deoxynojirimycin providing a prolonged hypoglycaemic effect. *Food Chem*. 2012;134(4):1823–1830. doi:10.1016/j.foodchem.2012.03.086
7. Faber ED, van den Broek LA, Oosterhuis EE, et al. The N-benzyl derivative of the glucosidase inhibitor 1-deoxynojirimycin shows a prolonged half-life and a more complete oral absorption in the rat compared with the N-methyl analog. *Drug Deliv*. 1998;5(1):3–12. doi:10.3109/10717549809052021
8. Sun Z, Yuan S, Zhao H, et al. Preparation and evaluation of 1-deoxynojirimycin sustained-release pellets vs conventional immediate-release tablets. *J Microencapsul*. 2017;34(3):293–298. doi:10.1080/02652048.2017.1321694
9. Ahmad R, Srivastava S, Ghosh S, et al. Phytochemical delivery through nanocarriers: a review. *Colloids Surf B Biointerfaces*. 2021;197:111389. doi:10.1016/j.colsurfb.2020.111389
10. Cui M, Liu Y, Liu Y, et al. Oral nano-formulations for endocrine therapy of endometrioid adenocarcinomas. *Biomed Pharmacother*. 2024;179:117328. doi:10.1016/j.biopha.2024.117328
11. Zhu MJ, Zhu SP, Liu QB, et al. Selenized liposomes with ameliorative stability that achieve sustained release of emodin but fail in bioavailability. *Chin Chem Lett*. 2023;34(1):107482. doi:10.1016/j.cclet.2022.04.080

12. Deng W, Xie Q, Wang H, et al. Selenium nanoparticles as versatile carriers for oral delivery of insulin: insight into the synergic antidiabetic effect and mechanism. *Nanomedicine*. 2017;13(6):1965–1974. doi:10.1016/j.nano.2017.05.002
13. Wilson KL, Murray J, Jamieson C, et al. Cyrene as a bio-based solvent for HATU mediated amide coupling. *Org Biomol Chem*. 2018;16 (16):2851–2854. doi:10.1039/c8ob00653a
14. Thabet Y, Elsabahy M, Eissa NG. Methods for preparation of niosomes: a focus on thin-film hydration method. *Methods*. 2022;199:9–15. doi:10.1016/j.ymeth.2021.05.004
15. Ren Y, Qi C, Ruan S, et al. Selenized polymer-lipid hybrid nanoparticles for oral delivery of tripterine with ameliorative oral anti-enteritis activity and bioavailability. *Pharmaceutics*. 2023;15(3):821. doi:10.3390/pharmaceutics15030821
16. Li Y, Cao Y, Tian YY, et al. 1-deoxynojirimycin ameliorates diabetic liver injury by regulating AMPK/SIRT1 and oxidative stress in db/db mice. *Endocr Metab Immune Disord Drug Targets*. 2025;25. doi:10.2174/0118715303327499250104221937
17. Jin M, Shen MH, Jin MH, et al. Hypoglycemic property of soy isoflavones from hypocotyl in Goto-Kakizaki diabetic rats. *J Clin Biochem Nutr*. 2018;62(2):148–154. doi:10.3164/jcbn.17-68
18. Li L, Chunta S, Zheng X, et al. β-Lactoglobulin stabilized lipid nanoparticles enhance oral absorption of insulin by slowing down lipolysis. *Chin Chem Lett*. 2024;35(4):108662. doi:10.1016/j.cclet.2023.108662
19. Ren Y, Nie L, Zhu S, et al. Nanovesicles-mediated drug delivery for oral bioavailability enhancement. *Int J Nanomed*. 2022;17:4861–4877. doi:10.2147/IJN.S382192
20. Honary S, Zahir F. Effect of zeta potential on the properties of nano-drug delivery systems - a review (part 1). *Trop J Pharm Res*. 2013;12 (2):255–264. doi:10.4314/tjpr.v12i2.19
21. Wu S, Sun K, Wang X, et al. Protonation of epigallocatechin-3-gallate (EGCG) results in massive aggregation and reduced oral bioavailability of EGCG-dispersed selenium nanoparticles. *J Agric Food Chem*. 2013;61(30):7268–7275. doi:10.1021/jf4000083
22. Wang L, Peng J, Wang X, et al. Carboxymethylcellulose sodium improves the pharmacodynamics of 1-deoxynojirimycin by changing its absorption characteristics and pharmacokinetics in rats. *Pharmazie*. 2012;67(2):168–173.
23. Oliveira ESC, Acho LDR, da Silva BJP, et al. Hypoglycemic effect and toxicity of the dry extract of Eugenia biflora (L.) DC. leaves. *J Ethnopharmacol*. 2022;293:115276. doi:10.1016/j.jep.2022.115276
24. Zhang L, Pan MY, Li T, et al. Study on optimal extraction and hypoglycemic effect of quercetin. *Evid Based Complement Alternat Med*. 2023;2023:8886503. doi:10.1155/2023/8886503
25. Yin J, Hou Y, Yin Y, et al. Selenium-coated nanostructured lipid carriers used for oral delivery of berberine to accomplish a synergic hypoglycemic effect. *Int J Nanomed*. 2017;12:8671–8680. doi:10.2147/IJN.S144615
26. Wang H, Shen Y, Zhao L, et al. 1-Deoxynojirimycin and its derivatives: a mini review of the literature. *Curr Med Chem*. 2021;28(3):628–643. doi:10.2174/0929867327666200114112728
27. Zhang Y, Li L, Chai T, et al. Mulberry leaf multi-components exert hypoglycemic effects through regulation of the PI-3K/Akt insulin signaling pathway in type 2 diabetic rats. *J Ethnopharmacol*. 2024;319(Pt 3):117307. doi:10.1016/j.jep.2023.117307
28. Liu Q, Li X, Li C, et al. 1-deoxynojirimycin alleviates insulin resistance via activation of insulin signaling PI3K/AKT pathway in skeletal muscle of db/db mice. *Molecules*. 2015;20(12):21700–21714. doi:10.3390/molecules201219794
29. Ren X, Guo Q, Jiang H, et al. Combinational application of the natural products 1-deoxynojirimycin and morin ameliorates insulin resistance and lipid accumulation in prediabetic mice. *Phytomedicine*. 2023;121:155106. doi:10.1016/j.phymed.2023.155106
30. Guan B, Yan R, Li R, et al. Selenium as a pleiotropic agent for medical discovery and drug delivery. *Int J Nanomed*. 2018;13:7473–7490. doi:10.2147/IJN.S181343
31. Li D, Yi G, Cao G, et al. Dual-carriers of tartary buckwheat-derived exosome-like nanovesicles synergistically regulate glucose metabolism in the intestine-liver axis. *Small*. 2025;2025:2410124. doi:10.1002/smll.202410124
32. Dai Y, Ding Y, Li L. Nanozymes for regulation of reactive oxygen species and disease therapy. *Chin Chem Lett*. 2021;32(9):2715–2728. doi:10.1016/j.cclet.2021.03.036
33. Summers HD, Rees P, Holton MD, et al. Statistical analysis of nanoparticle dosing in a dynamic cellular system. *Nat Nanotechnol*. 2011;6 (3):170–174. doi:10.1038/nnano.2010.277
34. Andrei II. Pharmacological inhibition of endocytic pathways: is it specific enough to be useful? In: Andrei I, editor. *Methods in Molecular Biology: Exocytosis and Endocytosis*. Vol. 440. Totowa, NJ: Humana Press; 2008:15–33.
35. Deng W, Wang H, Wu B, et al. Selenium-layered nanoparticles serving for oral delivery of phytomedicines with hypoglycemic activity to synergistically potentiate the antidiabetic effect. *Acta Pharm Sin B*. 2019;9(1):74–86. doi:10.1016/j.apsb.2018.09.009